ISSN online 2545-2819
ISSN print 0800-6377

Received: March 16, 2018
Revision received: Nov. 24, 2018
Accepted: Nov. 29, 2018

DOI: 10.2478/ncr-2018-0017

Influence of Cracking on Effects of Restrained Deformations in a Post-tensioned Concrete Bridge

Kimmo Jalonen, M. Sc.
Graduate researcher, Tampere University of Technology
Department of Civil Engineering
Korkeakoulunkatu 10, 33101, Tampere, Finland
k.k.jalonen@gmail.com

Joonas Tulonen, M. Sc.
Post-graduate researcher, Tampere University of Technology
Department of Civil Engineering
Korkeakoulunkatu 10, 33101, Tampere, Finland
joonas.tulonen@tut.fi

Anssi Laaksonen, Dr. Tech.
Professor, Tampere University of Technology
Department of Civil Engineering
Korkeakoulunkatu 10, 33101, Tampere, Finland
anssi.laaksonen@tut.fi

ABSTRACT
Imposed and restrained deformations cause stresses in continuous concrete bridges, and in analyses of the superstructure these stresses are usually reduced to some degree due to creep and cracking of concrete. This study examines cracking and redistribution of stresses in a bridge superstructure under the loads and load combinations used in the original bridge design. The subject of this study is a three-span post-tensioned continuous concrete cantilever beam bridge. The bridge was analysed with non-linear calculation utilising the general force method and

moment-curvature relationships. The analysis yielded the bending stiffness of the post-tensioned bridge superstructure as a function of bridge length under different loads. It was discovered that the secondary moment from prestressing force increased as the bending stiffness of the central span decreased due to cracking under external loads, which is not normally considered in design. The bending moment effects of linear temperature difference and support settlement decreased as expected as the superstructure bending stiffness decreased. The analysis provided new information on the effects of secondary moment from the prestressing force and on the difference between the cracked state and the linear elastic analysis of the concrete bridge superstructure.

Keywords: restrained deformations, concrete cracking, post-tensioned concrete, bridge

1. INTRODUCTION

The magnitude of the stresses from imposed and restrained deformations (later restrained deformations) depends on the bending stiffness of the superstructure, so it is clear that the stress level changes when the concrete superstructure cracks. This study considers cracking as the main factor affecting structural bending stiffness. The Finnish Transport Agency has an application guideline of the Eurocode [4] for determining the effect of cracking and creep on restrained deformations in bridge designs. In the corresponding Eurocode, EN 1992-2 [10], it is not instructed how the effects of cracking and creep on restrained deformations in bridge design should be considered. It has been found that a more detailed investigation of the subject is required in order to obtain certainty as to how much stresses from restrained deformations could be reduced in the design of a structure. In this article, a post-tensioned continuous beam bridge is examined, and further studies on a continuous reinforced beam bridge can be found in a master's dissertation [2] written on the topic.

Approximately 530 post-tensioned concrete bridges were built in Finland from 1970 to 1990. These bridges are now reaching an age when they need to undergo their first major renovations and repairs. The increase in vehicle loads has been substantial during their lifespan, so much so that the maximum vehicle is now 72 tonnes. More accurate calculations are needed in assessing the bearing capacity of bridges in order to avoid costly and unnecessary bridge strengthening operations. The results can also be utilised in the design of new bridges to produce better performing and more cost-effective structures. [2]

Generally, in bridge design, stresses from thermal loads and support settlement can be ignored in the ultimate limit state design of a reinforced concrete beam bridge, provided that critical structural components have sufficient rotation capacity. [3,4] Restrained deformation loads have to be included in the serviceability limit state design, but these can be sometimes reduced. The creep coefficient is used to calculate the extent to which the deformation loads of the elastic state are to be taken into account in designing a new bridge. The results of this study have been compared with the permitted reductions given in the Finnish Transport Agency's guidelines. [2]

2. ANALYSIS

2.1 The bridge

The selection of the post-tensioned bridge for this study was made in consideration of the general properties of all built bridges. A significant portion of the prestressed bridges in Finland have three spans. A bridge built in 2015 was selected for this study. The bridge is a post-tensioned continuous cantilever beam integral bridge. The bridge's prestressing steel is inside metal sheet ducts that are injected with cement grout. The horizontal and vertical geometry of the bridge is curved.

The studied bridge was chosen so that it would represent ordinary Finnish prestressed concrete bridges designed and built in the 21st century. The original bridge was designed in accordance with the Eurocodes and the Finnish guidelines for Eurocodes, [3,4] which are non-contradictory information that complement the Eurocodes. The choice to use an "ordinary" bridge was done so as to limit the amount of needed calculations, since comprehensive parametrisation of the calculation model was not conducted.

For this study, the geometry of the bridge was simplified in order to enable two-dimensional calculations by the general force method while utilising the symmetry of the superstructure. The bridge is assumed to be straight without end cantilevers in calculations (Figure 5) since it is difficult to take soil stresses into account in calculations based on the general force method. The span lengths of the bridge were 24.97 m + 31.17 m +24.97 m. Figure 1 shows the cross-sections of the bridge where effective width of the deck slab has been taken into account. The reinforcement bars and prestressing steel cables taken into account in the calculations are also shown.

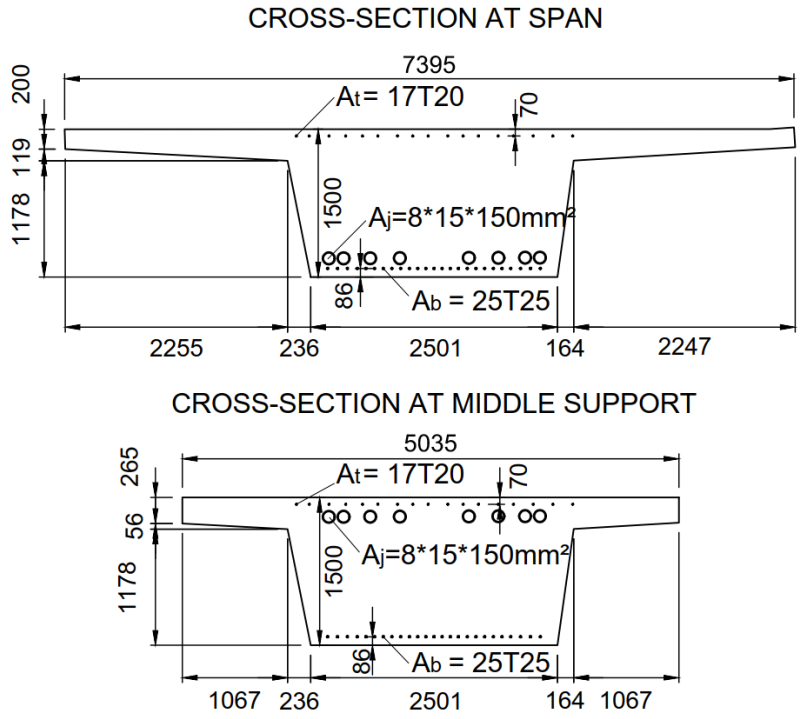

Figure 1 – Effective cross-section at spans and at middle supports.

2.2 Calculation steps

The analysis of the bridge is conducted with the following steps:

1. Moment-curvature relationships for bridge beam cross-sections are calculated
2. Calculation of the superstructure bending stiffness under all permanent and transient loads
3. Calculation of bending moments from linear temperature difference and secondary effects of prestressing force using calculated bending stiffness from step 2
4. Calculation of bending moments in a linear elastic situation, as would be done in design
5. Comparison of bending moments from non-linear and linear analyses

In the calculations of the moment-curvature relationships, it was assumed that planes remained plane and that the calculations were conducted with the actual geometries of the cross-sections, taking into account the effective widths of the flange. The effective widths of the cross-sections were determined according to SFS-EN 1992-1-1 [7].

49 moment-curvature relationships of cross-sections were calculated, with different reinforcement ratios and the location of the prestressing steel varying according to the bridge design drawings. Using moment-curvature relationships, it is possible to take into account e.g. flexural stiffness in a cracked and uncracked state with different load levels, complex cross-section shapes, non-linear material behaviour, etc. that have an influence on bending stiffness of the studied bridge superstructure. Furthermore, the moment-curvature relationship also contains information of the different material properties, the position and amount of steel and prestressing steel in a cross-section, cross-section dimensions and prestressing force. The material models used are from Eurocode SFS-EN 1992-1-1 and are presented in more detail in Section 2.4 [2].

Moment-curvatures are used as initial data in the analysis of the whole superstructure. The bending stiffness of every cross-section in a load-bearing superstructure can be calculated with moment-curvatures (Eq. 1) when the bending moment distribution of a superstructure has been calculated. In the first iteration of bending moment calculation, it is assumed that superstructure behaviour is linear elastic. After the bending moments have been calculated, the bending stiffness is recalculated and a second iteration is made. If the bending moments in middle supports are different than in the previous iteration, a new iteration will be made with a recalculated bending stiffness. This iteration will continue until the average moment of both middle supports is equal in subsequent iterations. The end of the iteration loop means that loads and bending stiffness are in equilibrium. Load-stiffness equilibriums are calculated with many live load positions and load history combinations in order to determine the most adverse bending stiffness degradation of the superstructure during its lifetime.

$$EI = \frac{M}{v''} \tag{1}$$

In this study the following loads have been used: dead loads, traffic loads, support settlement and linear temperature difference, as well as the tendon force and its secondary moment. The traffic load has been modelled with a more realistic vehicle shown in Figure 3 instead of the SFS-EN 1991-2 Load Model 1 (later LM1) [8] used in the original design of the bridge. The loads from the vehicle have been scaled so that the bending moments on this bridge would be approximately equal to those caused by LM1.

Bending moments from loads are calculated using the general force method [1]. The method allows arbitrary bending stiffness to be used anywhere in the superstructure. For instance, the general force method can be used in the analysis of a simple two-span beam with a uniform load and arbitrary bending stiffness, as shown in the following equations and in Figure 2.

$$a(x) = \int_0^L \frac{\bar{M}_1(x)^2}{EI(x)}\,dx \tag{2}$$

$$u(x) = \int_0^L \frac{M_0(x) * M_1(x)}{EI(x)}\,dx \tag{3}$$

$$X(x) = \frac{-u(x)}{a(x)} \tag{4}$$

$$M_t(x) = M_0(x) + X(x) * M_1(x) \tag{5}$$

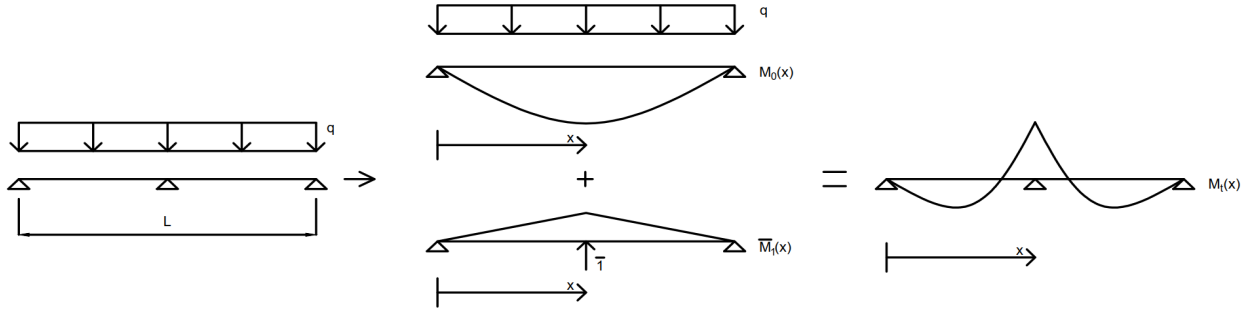

Figure 2 – Calculating the bending moment of a two-span continuous beam.

2.3 Loads

The loads and load combinations in this study were ones that are usually used in bridge design in Finland [3]. The loads in Finnish national guidelines [3,4] are based on Eurocode 1, while load combinations are based on Eurocode SFS-EN 1990 [9], though some of the recommended combination values have been modified nationally. Either traffic load or thermal load was chosen as the leading action in load combination. The structure was analysed with both serviceability limit state and ultimate limit state load combinations. In this study, only the results from the serviceability limit state are presented. The serviceability limit state quasi-permanent combination was also used to examine the effects of creep. Short-term and long-term prestress force losses were also taken into account. Serviceability limit state load combinations and load factors are shown in Table 1.

Support settlement was not present in the first calculation step, and for the second calculation step it was taken into account with factor 1.0. All other loads were included in every calculation step. Prestress force includes primary bending moment and secondary bending moment.

Table 1 – Serviceability state load combinations and combination factors [3].

	Characteristic combination (CHAR)	
Leading action	TEMPERATURE	TRAFFIC
Dead load	1.0	1.0
Tendon force	1.0	1.0
Support settlement	0/1.0	0/1.0
Linear temperature difference	1.0	0.6
Traffic load, UDL	0.4	1.0
Traffic load, TS	0.75	1.0

The vehicle load was modelled by vehicle AA 13/76 (Figure 3) [5], which is a vehicle determined for bridge assessment that corresponds to the largest truck allowed in public roads, to make the traffic load correspond more closely to actual vehicles than the LM1 that is used in design. The LM1 is by definition a design load model, and it was seen that the bending moment envelope along the bridge length would be more realistic with load model AA 13/76 used in the bridge assessment, since it is based on actual axle configurations of real vehicles. Peak moments from basic load model AA 13/76 are different from those of LM1, and this research takes design stresses of the structure into account, so the axle weights in load model AA 13/76 were scaled with scale factors so that the peak bending moments would match.

On the studied bridge were two road lanes, and two AA 13/76 vehicles were placed on both lanes. On one lane, the distance between the vehicles was set equal to the length of the side span. The vehicles on both lanes were driven simultaneously across the bridge. The stress induced by the vehicles was scaled so that it would be equally high as the impact of LM1 at the intermediate supports and mid-span. The calculated factors were different for maximum bending moment at the intermediate supports and the central span. The smallest factor was used in the calculations, for it does not overestimate the cracking of the structure. The impact of the LM1 varied depending on the used combination factors for combining the uniformly distributed load (UDL) for LM1 and the tandem system for LM1, as shown in Table 1.

When linear temperature difference was the leading action, the used scale factor was 0.92, and for traffic load leading action the used scale factor was 1.60. The linear structural model was used to determine the most critical traffic load positions, which were varied by ±4 metres in actual non-linear calculations. It was necessary to have variation of the traffic load positions because the calculations were non-linear, as well as to ensure that the maximum effect of the traffic load was uncovered.

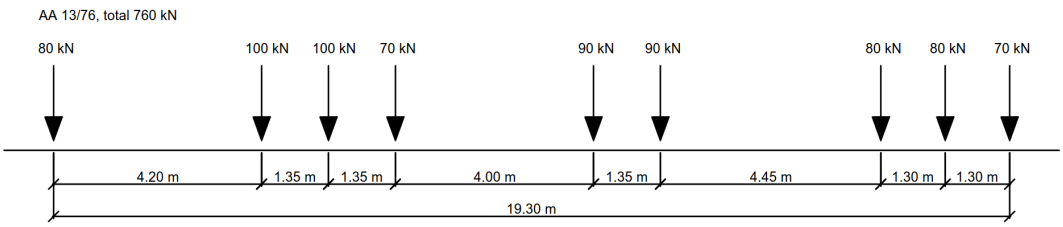

Figure 3 – Vehicle load model [5] used to calculate traffic load.

Support settlement and linear temperature difference were determined according to Finnish national guidelines [3]. Support settlement was 10 mm in each pier. Linear temperature

difference between the bottom and top of the structure was 9.9°C when the top of the structure was warmer and 8°C when the bottom of the structure was warmer. Calculation of the reduced values of linear temperature difference has been made according to Eurocode 1991-1-5 Table 6.1 and Table 6.2 according to the thickness of the bridge surface layer (110 mm). Tables 6.1 and 6.2 in Eurocode 1991-1-5 are the same in the Finnish national guidelines [3].

2.4 Materials

Material properties for reinforcing steel, prestressing steel and concrete specified in SFS-EN 1992-1-1 were used: for concrete Figure 3.3 in Ref. [7], for reinforcing steel Figure 3.8 3 in Ref. [7] and for prestressing steel Figure 3.9 3 in Ref. [7]. The bilinear stress-strain relationship was used to represent the behaviour of reinforcement and prestressing steel while the parabola-rectangle model was used for the concrete. No strain hardening of either prestressing steel or reinforcement was considered. Plastic elongation of reinforcement or prestressing steels was not limited when determining moment-curvature relationships of cross-sections. Table 2 shows the material strength and initial Young's modulus for each material used in the calculations. Characteristic material properties were used because they are typically used in designing the bridge in a serviceability limit state.

To take into account the change in tendon geometry and effective width of top flange, the moment-curvature relationships were calculated at several points in the beam's length. Figure 4 shows the moment-curvature relationship of the superstructure at the centre of the mid-span and at the intermediate support. Moment-curvature relationships of cross-sections were used to represent differing beam lengths of 0.3 m to 1.2 m. The centre of gravity of tendons and mean prestressing force were used in each cross-section. The location and amount of reinforcing steel, which are shown in Figure 1, remained unchanged for all calculated cross-sections.

The y-axes of the calculated moment-curvatures were modified so that the moment-curvature relationship would pass through point (0,0) of the graph. This shift was done because primary moment from prestress was already included as load in the calculation of total bending moment. Therefore, the magnitude of the shift was approximately the same as the primary moment from prestress. Figure 4 shows the calculated and shifted moment-curvature relationship at the centre of the mid-span and at the middle span.

Creep was not considered in the calculation of the moment-curvature relationships. Long-term loss of prestress force was assumed to be 15%.

Table 2 – Material properties.

Materials					
Concrete		Reinforcement steel		Prestressing steel	
f_{ck} [MPa]	35	f_{yk} [MPa]	500	f_{pk} [MPa]	1600
E_{cm} [GPa]	34	E_s [GPa]	200	E_p [GPa]	195
γ_c	1.35	γ_s	1.1	γ_p	1.1

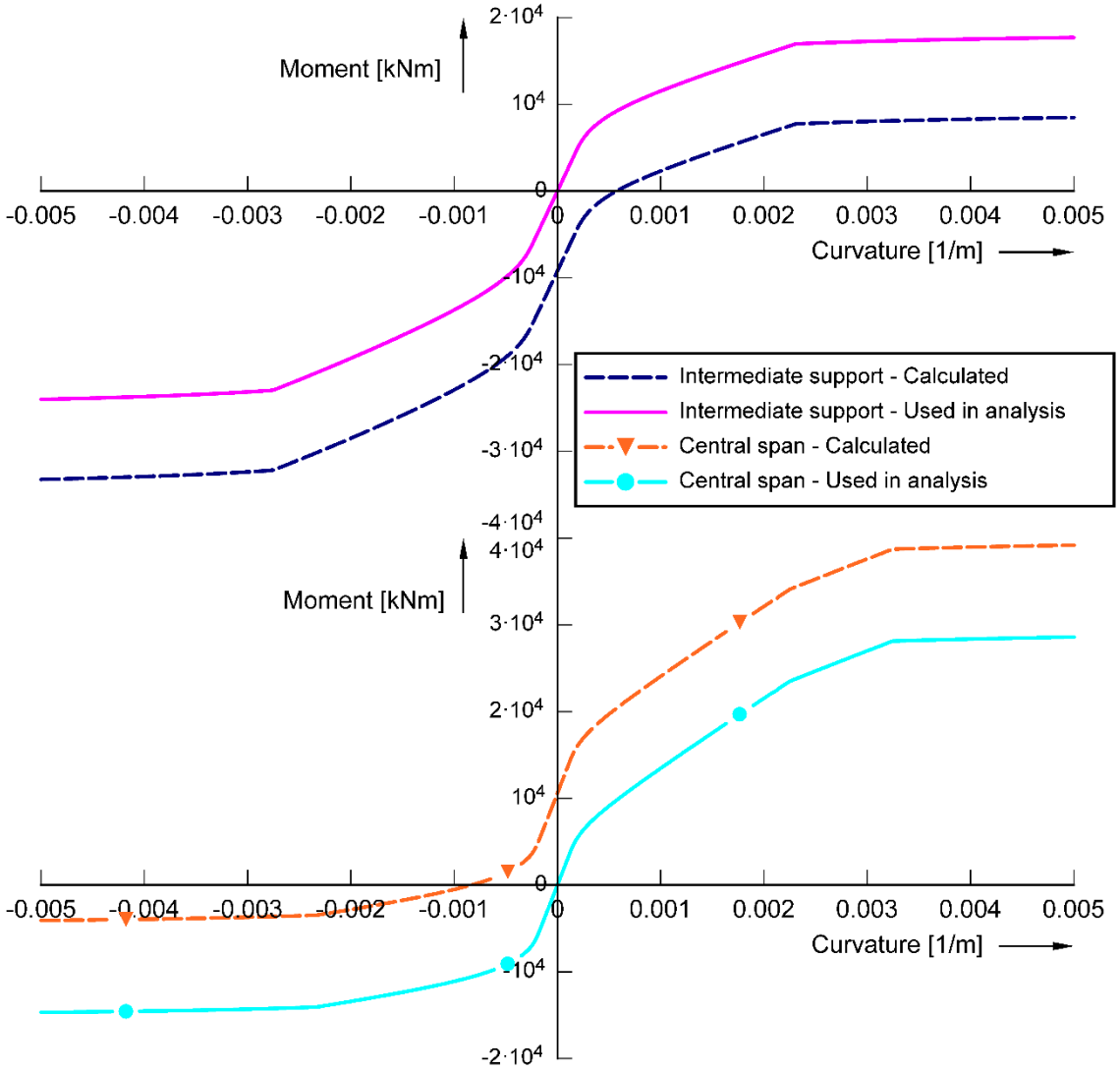

Figure 4 – Example of moment-curvature relationship at the middle of the central span and at the intermediate support.

2.5 Structural model

The bridge was modelled as a straight, continuous three-span beam bridge (Figure 5). In reality, the bridge was attached rigidly to all piers, but this was ignored in the model since the columns were slender. The calculation was further simplified by eliminating the end cantilevers from the model and adjusting the side spans to take advantage of symmetry. Because the cantilevers were eliminated from the beam model, bending moments representing the dead weight of the bridge ends were added to the ends of the beam model (Figure 5). Figure 6 shows the tendon geometry and prestress force used in the calculation.

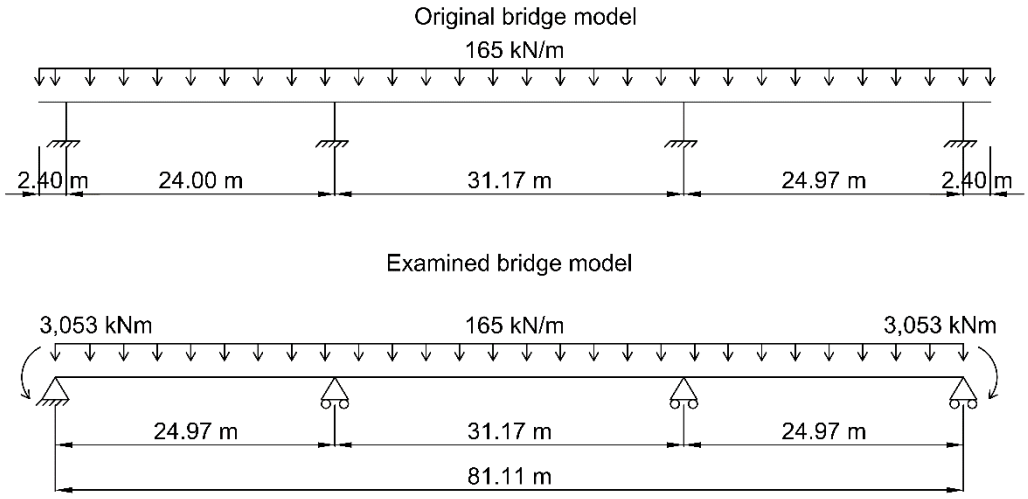

Figure 5 – Actual bridge geometry and geometry in the model.

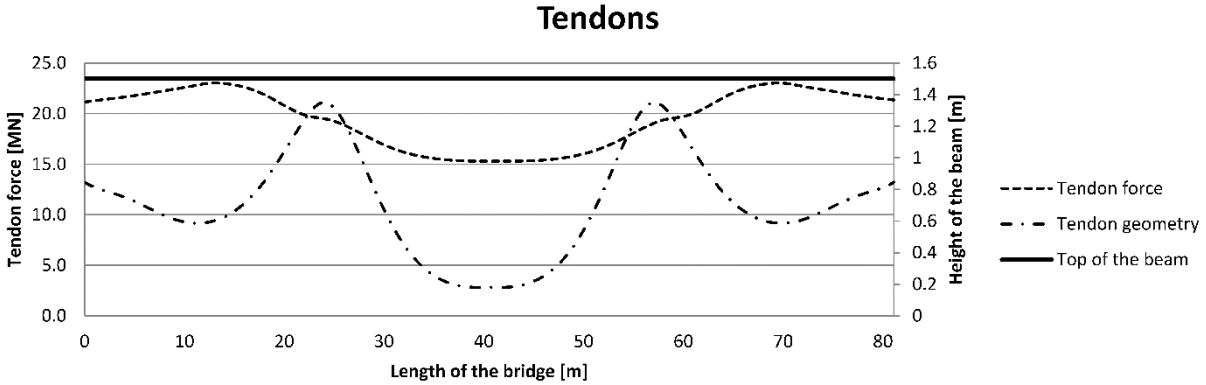

Figure 6 – Tendon geometry and prestress force used in the calculation.

The bending moment from the prestressing on the superstructure was calculated from Eq. 6

$$M_p = M_p^{(0)} + M_p', \tag{6}$$

where $M_p^{(0)}$ is the primary bending moment from the prestress force and M_p' is the secondary moment induced by restraining the primary deformations from prestress. The primary moment from the prestress force was derived from Eq. 7

$$M_p^{(0)}(x) = P(x) * e(x), \tag{7}$$

where $P(x)$ is prestress force and e(x) is the distance of the tendon from the centroid of the cross-section.

3. RESULTS

After each iteration, step calculations yielded residual bending stiffness of the bridge as a function of bridge length. Figure 7 shows residual bending stiffness as a function of bridge length in the characteristic combination where the traffic load was the leading action. Figure 7 shows that the largest change in the bending stiffness of the superstructure was at the middle of the central span.

The bending stiffness of the superstructure did not decrease compared to the initial situation at the intermediate supports or the side spans. The slight difference in the bending stiffness of the bridge superstructure between the elastic state and the characteristic combination resulted from the calculations of the moment-curvature relationship with non-linear materials. In a typical structural analysis of a bridge in its design state (linear elastic model with homogenous cross-section), the elastic bending stiffness does not include the effects of the reinforcement or the prestressing steel. Also, the stress-strain relationship of the concrete was different in the elastic state. These differences caused calculated bending stiffness to be slightly larger compared to the elastic state. Bending stiffness in the elastic state is shown for comparison, and the conclusions of the research are drawn from the analysis where change in bending stiffness is calculated with moment-curvature relationships.

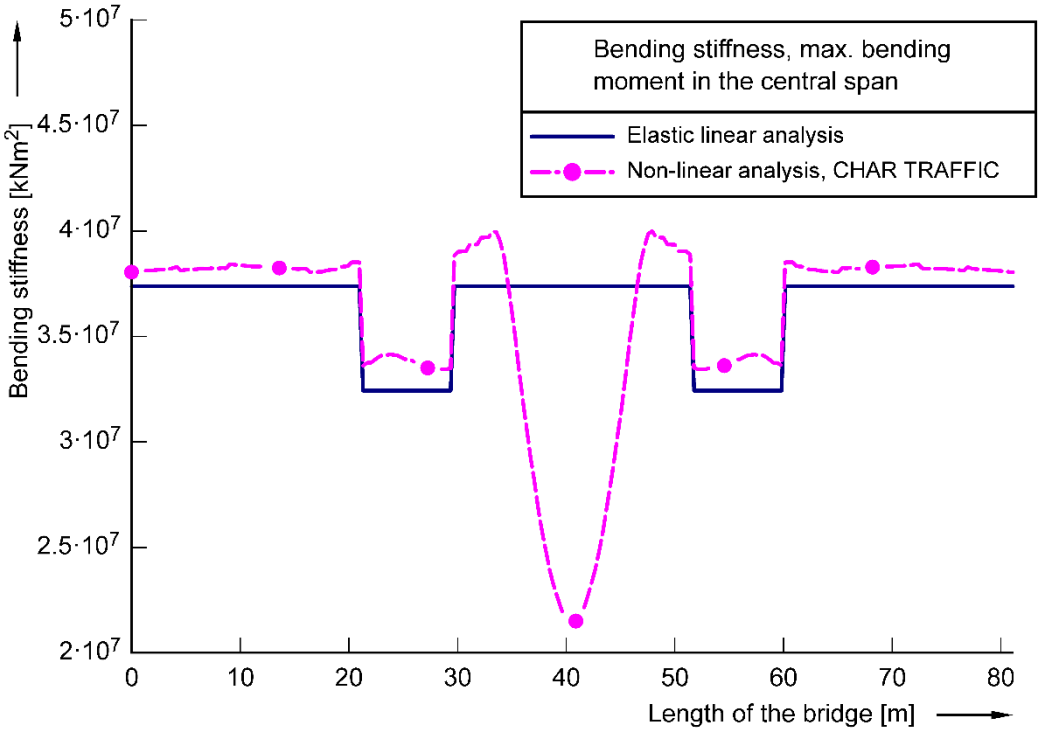

Figure 7 – Calculated bending stiffness and bending stiffness in an elastic state.

Decreasing the bending stiffness of the superstructure changed the bending moment distribution along the bridge length. Because the bending stiffness changed at the central span, the bending moments from external loads increased at intermediate supports and decreased at the central span. Bending moment redistribution was not significant at the side spans. Figure 8 shows the magnitude of the bending moments from external loads in characteristic combination.

Bending moments from support settlement and linear temperature difference decreased only slightly in the characteristic combination, while traffic load was the leading action as shown in Figure 9. The secondary moment from prestressing force increased by 0.5 MNm as the bending stiffness of the central span decreased more than in the rest of the superstructure. The combined effect of all restrained deformations was therefore larger than in the elastic state.

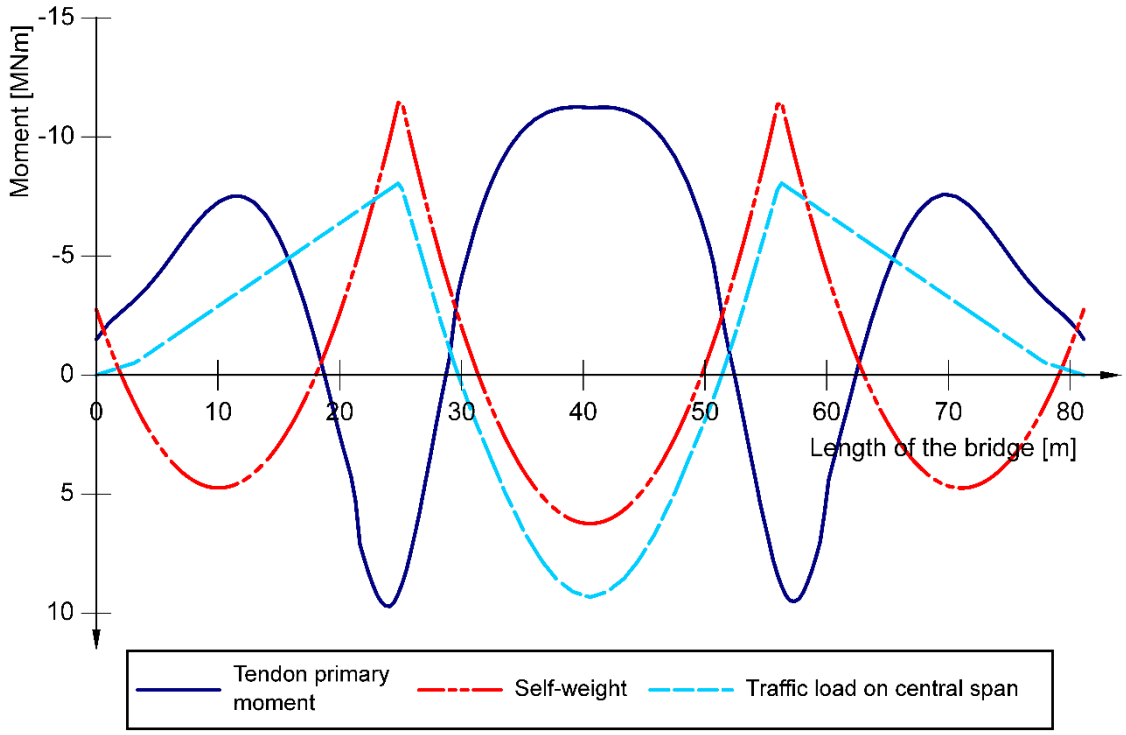

Figure 8 – Bending moments due to loads in characteristic combination of cracked bridge.

The abbreviation 'CHAR_Traffic_All' in Figure 9 and 10 means that non-linear calculations have been made with characteristic load combination while traffic load was the leading action and all loads were acting in the bridge. The abbreviation 'Elastic' means that calculations have been made using linear material properties while other assumptions were the same as above.

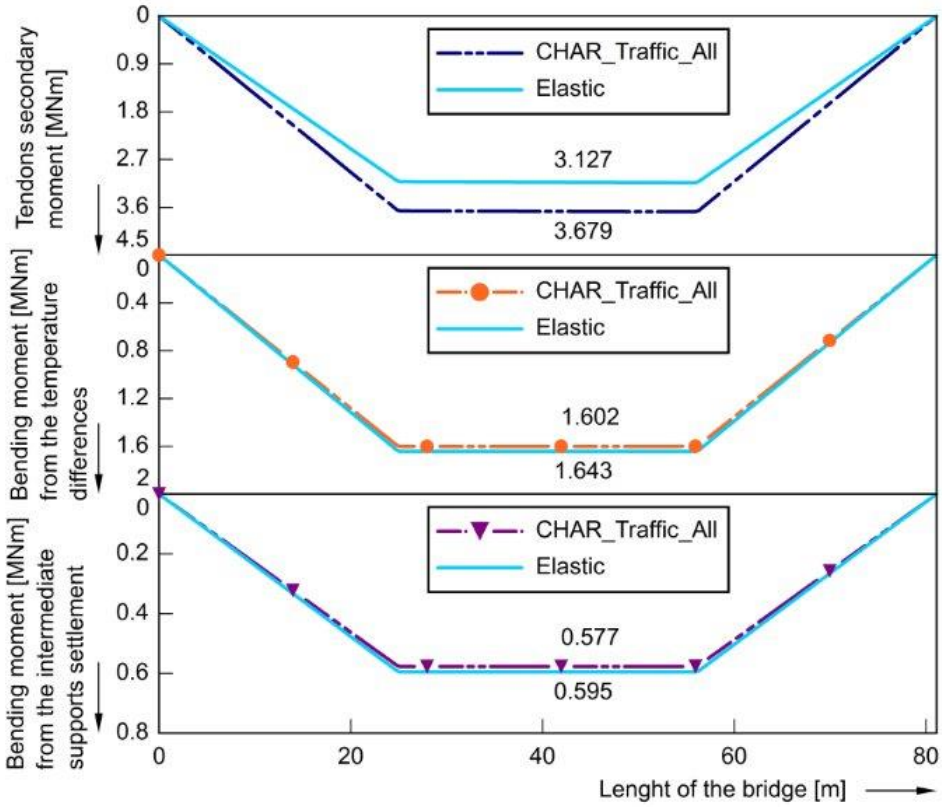

Figure 9 – Stresses from restrained deformations in the elastic state and after the stiffness degradation from loads.

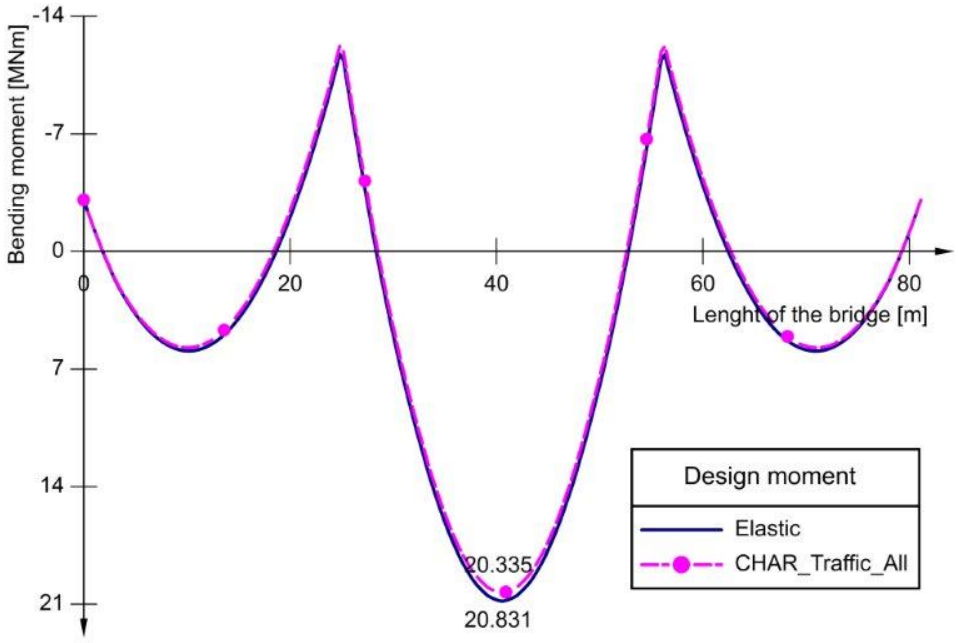

Figure 10 – Bending moments from all loads (excl. primary moment from prestressing force) in characteristic combination (with traffic load as leading action) and elastic state.

The difference between the elastic state and the characteristic combination with vehicle traffic load as the leading action is about 0.5 MNm at the middle of the central span. In the

characteristic combination, about 1 MNm of dead load and traffic load bending moments were transferred from the central span to the intermediate supports. Because the secondary moment of the tendon prestressing force increased at the same time, the difference of total bending moment decreased by only 0.5 MNm at the middle of the central span. Figure 10 shows that the changes were small compared to total bending moments.

In characteristic combination with temperature load leading actions, the bending moments from linear temperature difference were about the same as in the elastic state. When traffic load was the leading action, the bending moments from linear temperature difference were decreased because slightly more cracking occurred as shown in Table 3. In the characteristic combination, cracking of the bridge superstructure was significant only when traffic load was the leading action and maximum stresses were at the central span.

The values in parentheses in Table 3 and Table 4 are the results from calculations with serviceability limit state material models while loads were factored with ultimate limit state load factors. This calculation was done to provide results with loading that is closer to the maximum design load.

Table 3 – Stresses from linear temperature difference on cracked bridge in relation to elastic state (results where loads were factored with ultimate limit state load factors).

Max bending moment at	Loads included/ Leading action	THERMAL	TRAFFIC
Central span	All loads, excluding support settlement	1.03 (0.98)	0.99 (0.93)
	All loads	1.02 (0.95)	0.97 (0.91)
Intermediate supports	All loads, excluding support settlement	1.05 (1.05)	1.05 (0.98)
	All loads	1.05 (1.05)	1.05 (0.98)

Secondary bending moment of prestressing force from characteristic combination in relation to the elastic state is presented in Table 4. The results show that the secondary bending moment increased when the central span of the superstructure cracked under the characteristic combination of loads. Bending moment increased by up to 18% compared to the elastic state, which primarily occurred with load combinations where stresses in central span and cracking were larger than in intermediate supports. When observing secondary effects with load combinations where the maximum bending moment was at the intermediate support, the superstructure cracked at both the central span and intermediate supports which reduced the secondary moment from prestressing compared to the elastic state, and total bending moments remained essentially unchanged.

The results show that the relative change in bending stiffness of different parts of the bridge was the most important factor in determining the magnitude of effects from restrained deformations.

Table 4 – Secondary moment due to post-tensioning with design reinforcement in relation to elastic state (results where loads were factored with ultimate limit state load factors).

Max bending moment at	Loads included/ Leading action	THERMAL	TRAFFIC
Central span	All loads, excluding support settlement	1.04 (1.17)	1.13 (1.29)
	All loads	1.08 (1.22)	1.18 (1.34)
Intermediate supports	All loads, excluding support settlement	0.97 (0.98)	0.98 (0.89)
	All loads	0.96 (0.98)	0.98 (0.81)

Figure 9 shows that the secondary moment from prestressing resulted in considerably larger stresses than that caused by support settlement or linear temperature difference when the central span was cracked. If the total load on the central span was increased, the increase in secondary moment would also be larger, as shown in the results in parenthesis in Table 4. As the loading on the central span decreased, the stresses from the secondary moment also decreased. When bending stiffness is reduced uniformly in the length of the bridge superstructure, or in the central span and intermediate supports simultaneously, the tendon secondary moment remains unchanged compared to the elastic state. The behaviour of the secondary bending moment when bending stiffness changes due to cracking is entirely different compared to the effects from linear temperature difference. Currently, secondary bending moment from prestressing is often grouped with other restrained deformations, and its effects are relieved accordingly.

4. CONCLUSIONS

The structural design of a bridge is usually simplified by using linear elastic models, and the non-linearity in the actual behaviour of the structure is taken into account with empirical factors. In order to provide more information on this non-linear behaviour, a three-span post-tensioned concrete bridge designed in 2014 was studied with a structural model that would take into account the cracking of the concrete superstructure. The results of this study are summarised in Figure 11, which shows how the stresses of the bridge superstructure from restrained deformations change when the bending stiffness is decreased from loading in the central span only or in the central span and intermediate supports. The study revealed that, as central span bending stiffness decreased from loading, stresses from support settlement and linear temperature difference also decreased while secondary moment from prestressing was found to increase. When bending stiffness decreased from loading in the central span as well as in the intermediate supports, stresses from all restrained deformations decreased.

It is usual when designing a new bridge to reduce stresses caused by restrained deformations due to creep and cracking of concrete, but in this case the behaviour of the structure was opposite. The change in bridge bending stiffness occurred gradually, under normal design loads. If bending stiffness would decrease uniformly in the whole length of the superstructure, such as due to creep, the secondary moment from prestress would remain unchanged.

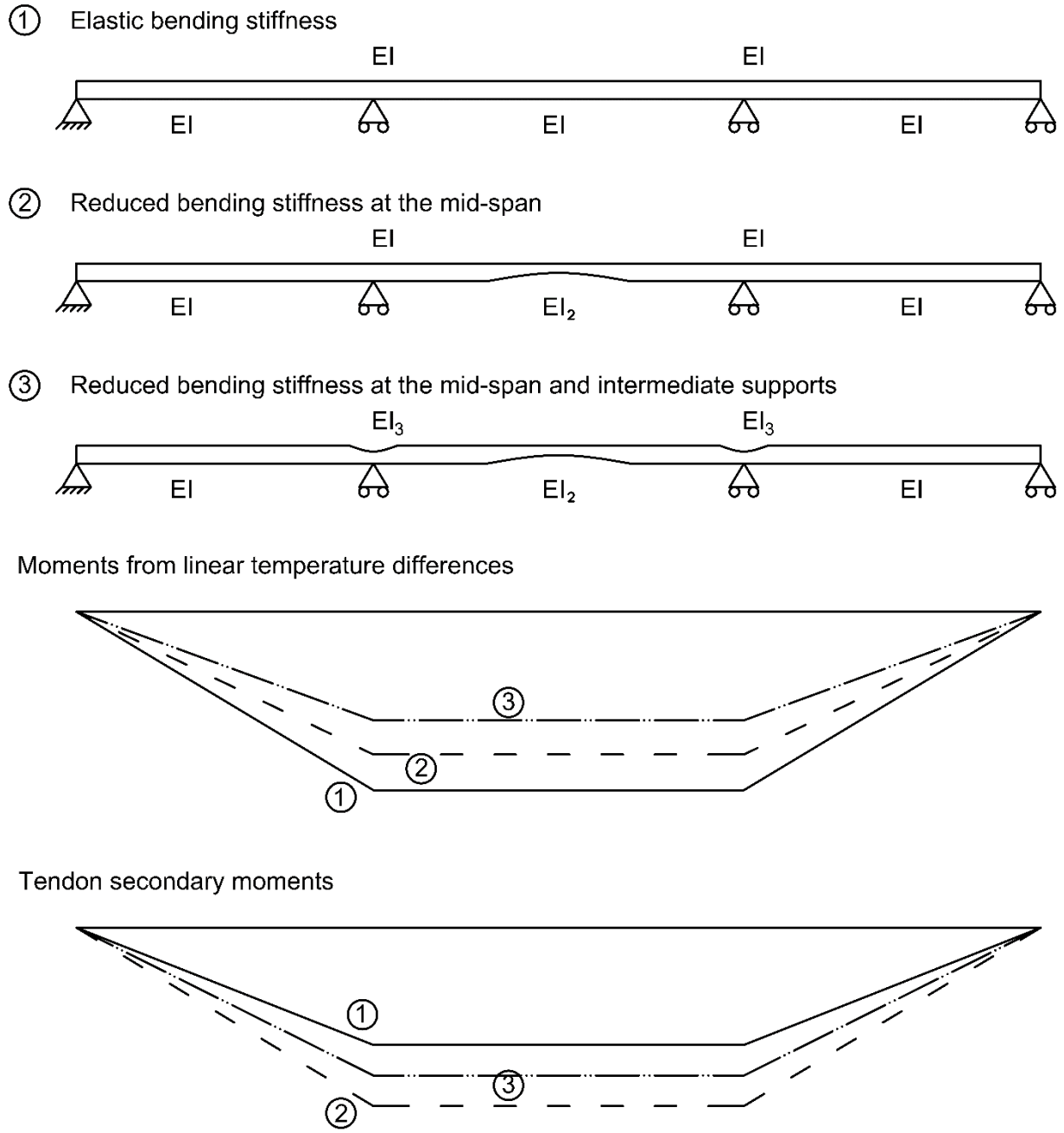

Figure 11 – Impact of change in bending stiffness on stresses from restrained deformations.

In the serviceability limit state, stresses from support settlement and linear temperature difference were not reduced as a result of cracking. Therefore, it would be justified to use stresses from linear elastic analysis when designing a new bridge. When creep was considered in the serviceability limit state, stresses decreased by up to 35% compared to the elastic state. The reduction in stresses was mainly due to the effect of creep on bending stiffness rather than cracking of the bridge. The effects of creep on the stresses were of an expected magnitude.

The increase in the secondary moment from prestress force was due to the cracking of the central span. The results indicate that the change in secondary moment from prestress depends on the location of the cracking of the superstructure.

This study on the behaviour of a post-tensioned bridge was conducted based on only one bridge cross-section with symmetrical spans, since the scope of the research was the effect of flexural cracking of the superstructure on the secondary bending moments in the case of an ordinary bridge structure. Parametrisation was excluded from the research, as the focus of this study was to test the calculation method and see how the structure would behave under some basic assumptions. The results of this study cannot be generalised due to these limitations. In the future, research should be done with parametrisation of several variables, including at least different reinforcement and span ratios, the variation in cross-section size and the variation in concrete strength classes. Results from future research should include generally applicable guidelines for design or for calculation of load-bearing capacity. The impact of cracking could also be examined with test loading of a continuous prestressed beam with a uniform load and support settlement.

ACKNOWLEDGEMENTS

The authors would like to thank the department of civil engineering of the Tampere University of Technology, Finland, that made this research project possible. They would also like to extend their appreciation to the Finnish Transport Agency for providing the financial support.

REFERENCES

1. Arnold A: ”Zum Einfluss der Zwangschnittgrößen aus Temperatur bei Tragwerken aus Konstruktionsbeton mit und ohne Vorspannung,” Dissertation, Dortmund Techn. Univ., Dortumund, Germany, 2008. (In German).
2. Jalonen K: “Imposed and restrained deformations on concrete bridge,” *Master Thesis*, Tampere University of Technology, Tampere, Finland, 2016. (In Finnish.)
3. Liikenneviraston ohjeita 24/2014. 2014. Eurokoodin soveltamisohje – Siltojen kuormat ja suunnitteluperusteet NCCI 1 (5.9.2014) (Guidelines of the Finnish Transport Agency). 24/2014. 2014. Guidelines for the application of the Eurocode – Bridge loads and basis of structural design NCCI 1 (5.9.2014)). Liikennevirasto, Helsinki, Finland. (In Finnish.)
4. Liikenneviraston ohjeita 25/2014. 2014. Eurokoodin soveltamisohje – Betonirakenteiden suunnittelu NCCI 2 (16.9.2014) (Guidelines of the Finnish Transport Agency 25/2014. 2014. Guidelines for the application of the Eurocode – Design of Concrete Structures NCCI 2 (16.9.2014)). Liikennevirasto, Helsinki, Finland, 2014. (In Finnish.)
5. Liikenneviraston ohjeita xx/2015 Siltojen kantavuuslaskentaohje (Kommenttiversio) (Guidelines of the Finnish Transport Agency xx/2015 Guidelines for assessment of bridges (Comment version)). Liikennevirasto, Helsinki, Finland, 2014. (In Finnish.)
6. SFS-EN 1991-1-5. Eurocode 1: Actions on structures. Part 1-5: General actions. Thermal actions. Suomen Standardoimisliitto ry. Finland, 2005.
7. SFS-EN 1992-1-1. Eurocode 2: Design of concrete structures – Part 1-1: General rules and rules for buildings. Suomen Standardoimisliitto ry. Finland, 2005.
8. SFS-EN 1991-2. Eurocode 1: Actions on structures. Part 2: Traffic loads on bridges. Suomen Standardoimisliitto ry. Finland, 2009.
9. SFS-EN 1990. Eurocode – Basis of structural design. Suomen Standardoimisliitto ry. Finland, 2010.
10. SFS-EN 1992-2. Eurocode 2: Design of concrete structures. Concrete bridges. Design and detailing rules. Suomen Standardoimisliitto ry. Finland, 2009.